

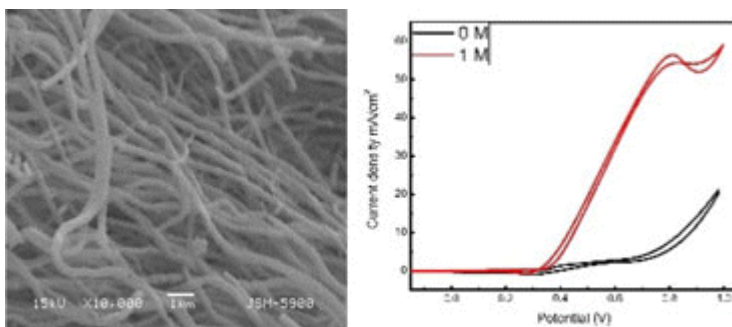
## BRIEF REPORTS

### 1. Cobalt/Chromium Nanoparticles-Incorporated Carbon Nanofibers as Effective Nonprecious Catalyst for Methanol Electrooxidation in Alkaline Medium

*Ibrahim M. A. Mohamed, Moaded Motlak, H. Fouad, Nasser A. M. Barakat*

1650049

Carbonization of electrospun mat composed of chromium acetate, cobalt acetate and poly(vinyl alcohol) at high temperature (900°C) produces Co/Cr-incorporated carbon nanofibers. The proposed nanofibers possess high electrocatalytic activity toward methanol electrooxidation as a clear peak of methanol oxidation appeared with corresponding current density of 56mA/cm<sup>2</sup>. The current density increases with the increase in methanol concentration up to 4.0M.

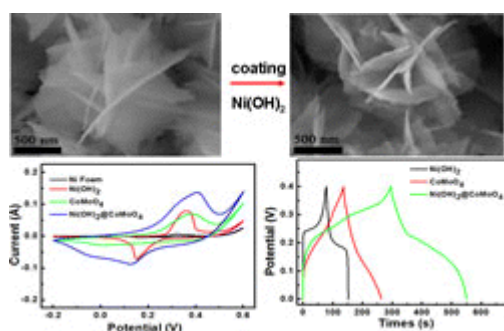


### 2. Construction of Hierarchical Ni(OH)<sub>2</sub>@CoMoO<sub>4</sub> Nanoflake Composite for High-Performance Supercapacitors

*Xueqing Li, Shuang-Yan Lin, Mingyi Zhang, Ge Jiang, Hong Gao*

1650050

Novel hierarchical Ni(OH)<sub>2</sub>@CoMoO<sub>4</sub> flower-like nanoflakes composite was successfully constructed by electrodepositing Ni(OH)<sub>2</sub> onto CoMoO<sub>4</sub> nanoflakes, which shows high areal capacitance and high capacitance retention. The high electrochemical performances can be attributed to the hierarchical nanoflakes structure and the synergetic effect between Ni(OH)<sub>2</sub> nanosheets and CoMoO<sub>4</sub> nanoflakes.

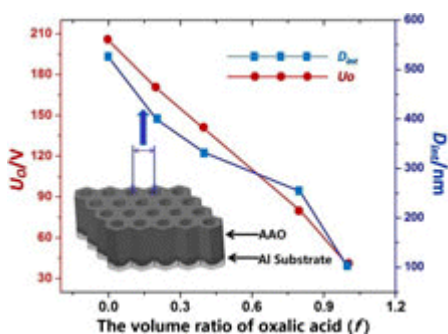


### 3. Preparation of Highly Ordered Anodic Aluminum Oxide Membranes with Wide-Range Tunable Pore Intervals in Mixed Electrolytes

Yi Chang, Zhiyuan Ling

1650051

The highly ordered anodic aluminum oxide membranes have been successfully prepared with pore interval from 100nm to 520nm in the mixed electrolytes. The linear relationship between optimal anodic oxidation voltage ( $U_o$ ) and oxalic acid volume percent ( $f$ ) in mixed electrolyte was reported. The characteristic of anodic oxidation current in the mixed electrolyte was also investigated.

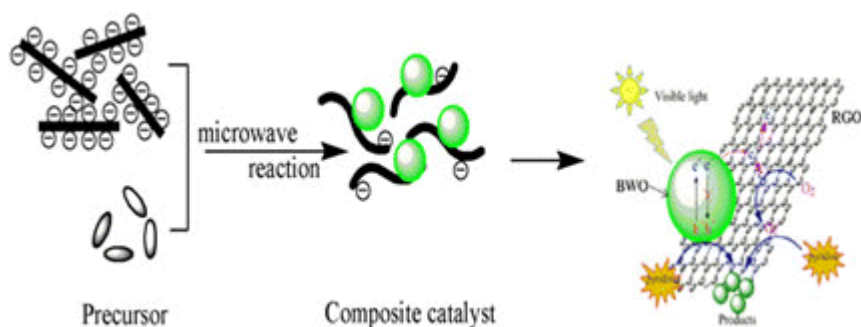


### 4. Ultrasonic-Microwave Synergistic Synthesis of RGO–Bi<sub>2</sub>WO<sub>6</sub> Photocatalyst with High Photoactivity for Basic Nitrogen Compounds in Light Oil

Ying Chen, Shenglun Ji, Tengfei Qiao, Shuang Miao, Yu Zhao

1650052

Bi<sub>2</sub>WO<sub>6</sub> is incorporated onto graphene sheets using an ultrasonic-microwave synergistic method to shorten the time of preparation of catalyst and graphene oxide which could be efficiently reduced under the microwave reaction. The graphene sheets not only function as a good substrate and stabilizer of Bi<sub>2</sub>WO<sub>6</sub> but they could also efficiently improve the electron transport and reduce the charge recombination.

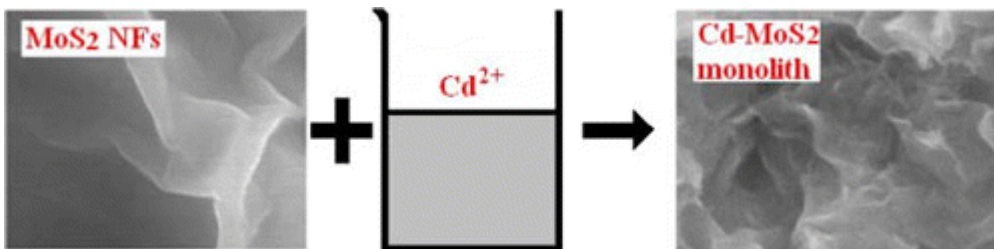


## 5. 3D Cd–MoS<sub>2</sub> Porous Monolith Fabricated Through a Self-Assembly Between Cd<sup>2+</sup> Cations and MoS<sub>2</sub> Nanoflakes

Tianhao Ji, Lifeng Zou, Hongkun Xia, You Wu

1650053

3D Cd–MoS<sub>2</sub> porous monolith was fabricated at room temperature using 2D MoS<sub>2</sub> nanoflakes as precursor and Cd<sup>2+</sup> cations through an interaction between the S atoms on the surface of the MoS<sub>2</sub> nanoflakes and the Cd<sup>2+</sup> cations. Such material exhibits relatively strong capacities in an adsorption of Rhodamine B molecules or Cu<sup>2+</sup> cations.

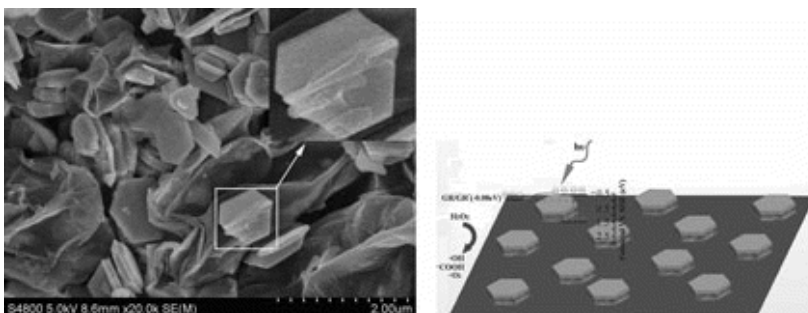


## 6. The Synthesis of CuS Hexagonal Nanosheet-Graphene for Use as a High Performance Photocatalyst

Bin Zeng, Yang Yin

1650054

Uniform deposition of CuS hexaplates nanosheets onto the graphene was synthesized. The samples possessed excellent visible light photocatalytic performance and a possible photocatalytic mechanism was proposed.

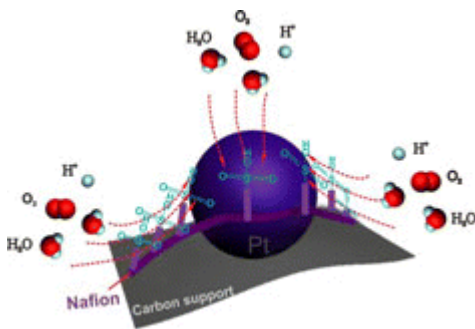


## 7. Enhancing the Specific Activity of Metal Catalysts Toward Oxygen Reduction by Introducing Proton Conductor

Kun Cheng, Xiaobo Liu, Wenqiang Li, Zongkui Kou, Shichun Mu

1650055

A perfluorosulfonic acid (Nafion®) stabilized Pt nanoparticles catalyst is fabricated through a simple colloidal route, which shows higher specific activity ( $I_s$ ) of oxygen reduction reaction (ORR), two times higher than that of the commercial Pt/C. We significantly confirm that the  $\text{SO}_3\text{H}$  groups in Nafion contribute directly to the much higher ORR activity. The mechanism can be ascribed to the  $-\text{SO}_3\text{H}$  groups, effectively promotes the transfer process of reaction species (e.g.  $\text{H}^+$ ,  $\text{H}_2\text{O}$ ), thus improving the triple-phase boundary.

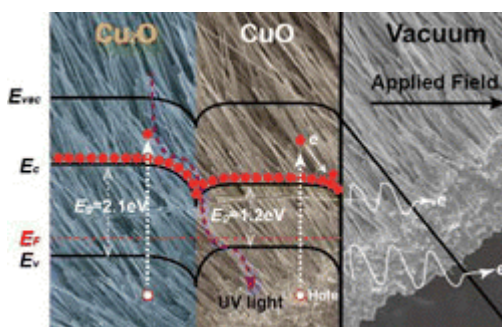


## 8. Enhanced Field Emission from UV-Illuminated CuO Nanowires Fabricated by Thermal Oxidation of Cu Film

Jiang Zhao, Debo Wang, Yue Chen, Qiu Jin, Guoqing Wang

1650056

CuO nanowire field emitter arrays were fabricated by a facile and effective thermal oxidation method. Simple UV illumination treatment was found to effectively enhance the field emission ability of CuO nanowire arrays. The energy-band diagram of CuO nanowire arrays in an applied field under UV illumination was used to explain the possible reasons for improving of field emission properties.

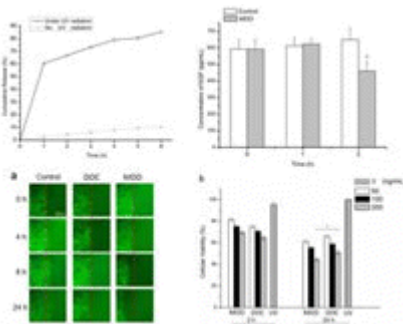


## 9. P(BA-co-HBA) Coated Fe<sub>3</sub>O<sub>4</sub>@ZnO Nanoparticles as Photo-Responsive Multifunctional Drug Delivery Systems for Safer Cancer Therapy

Xiao Huang, Xi Zheng, Caixia Yi, Shuanghong Yin

1650057

A novel photo-responsive multifunctional drug delivery not only can realize controlled DOC release but also adsorb EGF, which shows higher inhibition to CNE.

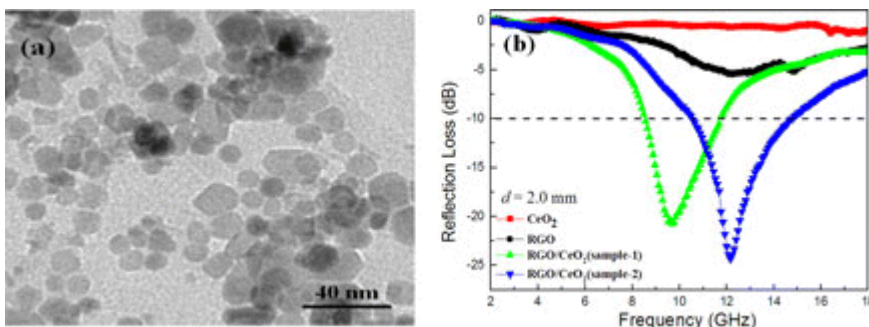


## 10. Enhanced Microwave Absorption Properties of CeO<sub>2</sub> Nanoparticles Supported on Reduced Graphene Oxide

Qing Yin, Honglong Xing, Ruiwen Shu, Xiaoli Ji, Dexin Tan, Ying Gan

1650058

CeO<sub>2</sub> well-dispersed nanocrystals, anchored on the reduced graphene oxide hybrid composites, were synthesized by a facile hydrothermal method. Microwave absorption properties measurement shows that the introduction of reduced graphene oxide significantly enhances the microwave absorption intensity of CeO<sub>2</sub> nanocomposites, and the bandwidth of reflection loss is also broadened. The concentration of oxygen vacancy defects plays a key role in the enhanced microwave absorption properties.

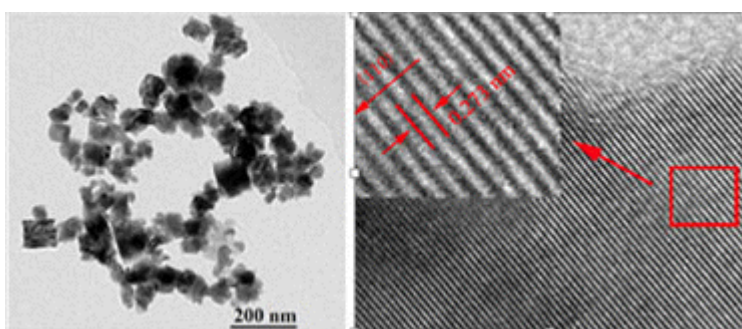


## 11. Molten Salt Synthesis of Strontium-Doped Lanthanum Manganite Nanoparticles with Enhanced Catalytic Performance for Toluene Combustion

Yingliang Tian, Wencai Liu, Yongqiang Lu, Shibing Sun

1650059

In the current study,  $\text{La}_{1-x}\text{Sr}_x\text{MnO}_{3-\delta}$  (LSMO) and  $\text{LaMnO}_{3+\delta}$  (LMO) nanoparticle catalysts have been fabricated by a one-step molten salt route. The doping of Sr may be conducive to better crystallization or easier growth of crystal. The as-synthesized LMO and LSMO samples exhibited high catalytic activities for the combustion of toluene, and the partial substitution of lanthanum by strontium had a promoting effect on the catalytic performance.



## 12. Uniform DNA Biosensors Based on Threshold Voltage of Carbon Nanotube Thin-Film Transistors

Yanyan Deng, Min Zhang, Fang Yuan, Zigang Li, Wenyu Zhou

1650060

Uniformity is a key parameter and a prerequisite to assure the accuracy of biosensor devices. Highly uniform CNT-TFTs with a standard deviation of  $V_{th}$ , as small as 0.04, were achieved in this paper. Based on this high uniformity, the CNT-TFTs are used as ultra-sensitive 5-hmC detecting devices, for the first time, by facile process. A reproducible and stable shift on  $V_{th}$  of CNT-TFTs was observed after the 5-hmC detection due to the charge injection.

